

Extent of pollution in planet-bearing stars

S.-L. Li^{1,2}, D. N. C. Lin^{2,3}, and X.-W. Liu^{1,3}

¹*Department of Astronomy, Peking University, Beijing 100871, China*

²*Department of Astronomy and Astrophysics, University of California, Santa Cruz, CA 95064, USA*

³*Kavli Institute for Astronomy and Astrophysics, Peking University, Beijing 100871, China*

ABSTRACT

Search for planets around main-sequence stars more massive than the Sun is hindered by their hot and rapidly spinning atmospheres. This obstacle has been sidestepped by radial-velocity surveys of those stars on their post-main-sequence evolutionary track (G sub-giant and giant stars). Preliminary observational findings suggest a deficiency of short-period hot Jupiters around the observed post main-sequence stars, although the total fraction of them with known planets appears to increase with their mass. Here we consider the possibility that some very close-in gas giants or a population of rocky planets may have either undergone orbital decay or been engulfed by the expanding envelope of their intermediate-mass host stars. If such events occur during or shortly after those stars' main sequence evolution when their convection zone remains relatively shallow, their surface metallicity can be significantly enhanced by the consumption of one or more gas giants. We show that stars with enriched veneer and lower-metallicity interior follow slightly modified evolution tracks as those with the same high surface and interior metallicity. As an example, we consider HD 149026, a marginal post-main sequence $1.3-M_{\odot}$ star. We suggest that its observed high (nearly twice solar) metallicity may be confined to the surface layer as a consequence of pollution by the accretion of either a planet similar to its known 2.7-day-period Saturn-mass planet, which has a $70-M_{\oplus}$ compact core, or a population of smaller mass planets with a comparable total amount of heavy elements. It is shown that an enhancement in surface metallicity leads to a reduction in effective temperature, an increase in radius and a net decrease in luminosity. The effects of such an enhancement are not negligible in the determinations of the planet's radius based on the transit light curves. Finally, we show that the extent of pollution can be inferred directly from high precision distant determinations and transit observations.

Subject headings: planetary systems

1. Introduction

In the radial-velocity search for planets around nearby main sequence FGK dwarf stars, it is well established that the detection probability of Jupiter mass gas giant planets increases rapidly with the metallicity of the target stars (Gonzalez 1997; Fischer & Valenti 2003; Santos et al. 2003). There are two scenarios for this observational correlation: 1) the host stars of planetary systems are polluted by infalling planets (Sandquist et al. 2002), 2) gas giant planets are preferentially formed around metal-rich stars (Ida & Lin 2005).

For the first (pollution) scenario, there are many potential avenues which may lead to planetesimal or protoplanet accretion by their host stars. For example, during the epoch of protoplanet formation, planetesimals and protoplanets undergo orbital decay as they interact with their nascent disks (Goldreich & Tremaine 1980; Ward 1984; Lin & Papaloizou 1986). Unless the migration of those entities can be stalled by their interaction with their host stars (Lin et al. 1996), they have a tendency to be accreted (Ida & Lin 2004). Since T Tauri stars have deep convective regions, any accreted metal-rich protoplanets during the first few Myr formation time of the star are dissolved in the envelope and the excess metals are mixed by convection and homogenized throughout the envelope.

On the time scale of ~ 30 Myr, the convection zone of a solar-type star is reduced to contain only the top 2% of the total stellar mass and $\sim 100M_{\oplus}$ heavy elements (Ford et al. 1999). This time scale is shorter and the total mass of the convection zone is smaller for F than for G dwarf stars. In systems which contain eccentric gas giants, the disk depletion process also leads to a sweeping secular resonance (Ward et al. 1976; Heppenheimer 1980; Ward 1981; Nagasawa & Ida 2000; Nagasawa et al. 2001) which can cause the residual planetesimals to migrate towards their host stars (Nagasawa et al. 2005; Zhou et al. 2005) and excite the gas giants' eccentricities (Nagasawa & Lin 2005). After the gas depletion, long term dynamical instability can also lead to orbit crossing and close encounters which can scatter the residual planets into their host star (Chambers 2001). Finally, most stars form in clusters which are eventually disrupted under Galactic tides. Stellar encounters can also lead to perturbations which can destabilize planetary systems and induce residual planetesimals bombardment onto their host stars (Adams et al. 2003). When those planets and planetesimals enter the atmosphere of their host stars, they become disintegrated as a consequent of Rayleigh-Taylor and shearing instabilities (Sandquist et al. 2002). The metal-enriched planetary debris rapidly dissolves and becomes mixed with the gas in the convective envelope near the stellar surface. In G dwarfs, this process can significantly enhance the observable metallicity on their surface.

For the second (threshold-core-accretion) scenario, gas giant planets form more prolifically around metal-rich stars. Presumably all the contents of those stars were accreted via

proto-stellar disks. Heavy elements first condense into grains which not only evolve through cohesive and disruptive collisions with each other but also undergo orbital decay as a consequence of gas drag. The efficiency of grain-planetesimals conversion increases with the metallicity of the disk because both collision rate and orbital decay time scale also increase with the disk metallicity (Supulver & Lin 2000). Gravitational instability in dust layers is also more likely to occur in metal rich disks (Sekiya et al. 1983; Youdin & Shu 2002). However, the threshold metallicity for the onset of gravitational instability may be considerably larger than those of the most metal-rich stars (Garaud & Lin 2004). The additional planet-building material also enhances the growth rate of planetesimals and increases the asymptotic isolation mass of proto-planetary embryos around metal-rich stars and therefore promotes the emergence of gas giant planets (Ida & Lin 2005, 2007).

A direct method to distinguish between these two scenarios and to quantitatively determine the extent of heavy element pollution is to observationally deduce the metallicity dispersion among similar mass stars within a given open cluster. The observed chemical homogeneity among solar-type stars in the Pleiades and IC 4665 clusters (Wilden et al. 2002; Shen et al. 2005) places a stringent upper limit ($< 10M_{\oplus}$) on the added heavy elements that they might have acquired after they enter the main sequence evolutionary track. In addition, the formation of planets requires proto-stellar and debris disks to retain at least comparable amount of heavy elements ($\sim 100M_{\oplus}$) as that contained in the solar system planets (Ida & Lin 2004). The observed chemical homogeneity among the cluster stars challenges this requirement. However, despite several attempts to search for planets in the Hyades (Guenther et al. 2005), only one planet has been found around one star (Sato et al. 2007). Therefore, the stringent upper limit in the metallicity dispersion does not provide sufficient information to place an upper limit on the amount of pollution onto the cluster stars.

A more subtle differential comparison is to search for any correlation between the metallicity and mass of planet-bearing field stars. Since the mass of the convective envelope of solar-type stars decreases with stellar mass, extensive pollution should lead to a correlation between the spectral type and the surface metallicity (Laughlin & Adams 1997). Among the known GK dwarf stars harboring planets, the lack of any spectral class-metallicity correlation has been cited as evidence that the late accretion of planets and planetesimals cannot account for the preferential association of planets with metal-rich stars (Fischer & Valenti 2005). Quantitatively, it limits the amount of late planetesimal/planet accretion to be less than the total heavy elements contained within the surface convection zone of planet-bearing stars. For planet-bearing main-sequence host stars (mostly G and K dwarfs), the mass of their convective envelope is $\gtrsim 10^{-2}M_{\odot}$. So to yield any observable variations in their surface metallicity, pollution of well over $100M_{\oplus}$ metals are needed after the stars have begun their main sequence evolution.

Although, the elevated metallicity of planet-bearing solar type stars can be easily accounted for by the threshold-core-accretion scenario, pollution at some level is unavoidable unless the planet formation process is highly efficient in retaining all the planet building blocks. In the outer solar system, the long-term perturbation of Jupiter and Saturn has resulted in the outward scattering of most residual planetesimals and the formation of the Kuiper-belt objects and Oort Clouds. Nevertheless, at least a fraction of this population (a few M_{\oplus}) is also scattered inward to form the terrestrial planets and to be accreted by the Sun. Due to observational selection effects, most of the known extra-solar planets have periods less than those of the gas giants in the solar system. In those relatively compact planetary systems, the inward-scattered fraction is likely to be larger than that in the solar system because close planetary encounters are less able to provide an adequate dynamical boost to the planetesimals’ orbital energy for them to overcome the steeper stellar gravitational potential. The determination of this fraction is particularly important in the calibration of the efficiency of planet-formation process and the assessment on the fraction of stars which contain gas giant planets.

Another motivation to search for evidences of planet consumption is the theoretical expectation of a larger-than-observed population of close-in gas giant planets (Ida & Lin 2005, 2007). Although type II migration can account for the overall origin of the short-period planets, their survival requires halting mechanisms such as planet-star interaction for those with close-in orbits and disk depletion for those with intermediate (a week to a year) periods. The period distribution of these planets requires the disruption of a significant fraction of gas giants which migrated to the stellar proximity. Around systems with known close-in planets, there is an elevated possibility of several prior generation gas giants which have migrated to even closer to their host stars. These “missing” planets may either have migrated directly into their host pre-main-sequence host stars or were halted initially and then resumed their orbital decay on a much longer tidal evolution time scale. The latter scenario would imply a general decline in the fraction of stars with close-in gas giants as the systems age. Again, establishing evidence for gas giant planet consumption is important in providing valuable clues on the dynamical evolution of planetary systems.

Ideally, constraints on the extent of protracted metallicity pollution is best placed on the intermediate-mass (earlier than F8) planet-bearing stars. The accretion of a Jupiter-like planet or a few M_{\oplus} planetesimals during the main sequence life span of these candidate stars would significantly enhance the metallicity of their shallow convective envelopes. However, atmospheres of these stars are hotter than those of the solar-type stars and they often have rapid spins. The former effect prevents the formation of many useful spectroscopic lines whereas the latter introduces considerable Doppler broadening. Both effects introduce challenges to the radial velocity surveys for planetary companions around high-mass stars.

Consequently, there were very few F stars in the original sample based on which the spectral class-metallicity correlation was established.

More recently, searches for planets around massive stars have shifted to target such stars after they have evolved onto their sub-giant and giant tracks and become G-giant stars. During this post-main-sequence phase, the atmosphere of these stars becomes cool with relatively slow spins. Preliminary surveys indicate that the fraction of these relatively massive G giant stars with planets may be higher than that around the solar-type G dwarf main sequence stars (Sato et al. 2007; Johnson et al. 2007; Dollinger et al. 2007). In addition, all of these planet-bearing stars have metallicity comparable to that of the Sun. Based on the lack of any obvious metallicity-dependence in the frequency of planet-bearing G giant stars, in contrast to the well-known metallicity-planet frequency correlation amount the G-dwarf stars, Pasquini et al. (2007) suggest that the planetary consumption may be a major cause for this dichotomy. In this scenario, 1) the high surface metallicity among the main sequence stars is mainly due to planet consumption and 2) the surface metallicity of planet-bearing stars decreases during their post main sequence evolution as their convective envelopes steepen and become more diluted.

There are some supporting evidences for planet consumptions among the G giant stars. There is an apparent lack of short-period gas giant planets around these stars despite the fact that they are much easier to be detected. In contrast, several-dozen known planets around main-sequence stars have periods less than 5 days, with some as short as 1 day. The post-main-sequence expansion of their host stars' envelope, the star-planet tidal effect may promote the orbital decay of close-in gas giants by the excitation of both Hough and inertial waves (Ogilvie & Lin 2007). If such a process can lead to the consumption of short-period gas giants, the accreted planetary debris would be retained near the surface layer above the radiative interior. Eventually, the stellar envelope engulfs the orbits of the close-in planets, induces their orbital decay and disruption (Livio & Soker 2002). The mass contained in the convection zone of the post-main-sequence stars increases with the expansion of their photospheric radius. When these stars enter the sub-giant phase, there would be sufficient mass in the convective envelope to homogenize and reduce their surface metallicity to their interior solar values. Nevertheless, between these two epochs, *i.e.* shortly after they have evolved off the main sequence but before they have entered the sub-giant track, the prior consumption of very close-in metal-rich gas giants or a population of rocky planets around sufficiently massive stars may lead to noticeable metallicity enhancement near their surface layers.

In this paper, we identify a planet-bearing star, HD 149026, as a transitional (between main-sequence turnoff and the subgiant branch) system. The host of this system is a post

main sequence $1.3-M_{\odot}$ star with nearly twice solar metallicity and it has a $P = 2.7$ day period Saturn-mass planet (HD 149026b) with a 70-earth-mass core. In a companion paper (Li et al. 2007), we propose that the large core structure of this planet was acquired through planetary mergers after it has migrated to the proximity of HD 149026. In this scenario, some debris material and residual planetesimals are expected to be scattered into the host star by such a close-in planet. The migration of HD 149026b may also have induced the orbital decay of planets and planetesimals along its migration path (Zhou et al. 2005). Long term dynamical instability could also have led to planet accretion onto the host star. Based on these anticipations, we identify HD 149026 to be an ideal star to study the effect of pollution.

The present-day convection zone of HD 149026 is an order of magnitude less massive than that of the Sun ($0.02 M_{\odot}$). The consumption of a few earth mass of residual planetesimals, embryos, or a metal-rich gas giant can easily increase the metallicity of this thin layer from the solar value to the observed one ($[\text{Fe}/\text{H}] \sim 0.36$). We briefly describe the method for computing the effect of pollution in §2. We present the impact of the stellar structure due to planetary accretion in §3 and the effect on the stellar evolution during the main-sequence turn off of HD149026. We show that within the range of the present observational uncertainties, the internal $[\text{Fe}/\text{H}]$ of HD 149026 may be comparable to that of the Sun. We also show that a surface pollution of this star may modify its post-main-sequence evolutionary track and its present-day mass-radius relation. Based on these stellar models, we outline a set of self-consistent observational tests which may be used to check the merger and stellar pollution hypothesis in §5. This test is also important to place a more precise determination of the planetary radius and the mass of its core. Finally, we summarize our results and discuss their implications in §6.

2. Computational method

We construct stellar models with the Eggleton stellar evolution code (Eggleton 1971, 1972). It is based on an 1-D Henyey scheme with adaptive mesh. The input physics has been updated by Pols et al. (1995) and implemented by Sandquist et al. (2002). It includes combination of OPAL opacity for stellar interior (Iglesias & Rogers 1996) and low-temperature opacities for the surface (Alexander & Ferguson 1994), combination of SCVH (Saumon et al. 1995) and OPAL (Rogers 1994) equations of state, and nuclear reaction rates (Bahcall et al. 1995). Chemical diffusion is included, using the method of Thoul et al. (1994). Convection is treated using the standard mixing-length theory and semi-convective mixing is incorporated in a diffusive manner. By calibrating solar model with the observational data of the present sun, we obtain the ratio of mixing length to the pressure scale height $\alpha = 1.933$. We find

satisfactory agreement when comparing the radius of the convection zone base of our solar model with the observed value from solar p-mode spectrum (Christensen-Dalsgaard et al. 1991).

The code has been adapted to allow for the non-homogeneous metallicity for polluted stellar models. In previous investigations on the effects of stellar pollution (i.e. Laughlin & Adams 1997; Dotter & Chaboyer 2003; and Cody & Sasselov 2005), stellar models are constructed based on the assumption that the high-metallicity material accreted by the star is fully mixed in the stellar convective envelope. This approximation is adequate for solar-type stars since all debris are dissolved during their passage through the stellar outer convective layers. HD 149026 is an F-type star with a very shallow convective layer with a total mass $\sim 0.003 M_{\odot}$ in hydrogen gas. If the surface convective layer is homogeneous and has an $[\text{Fe}/\text{H}]$ as observed, its total mass of heavy elements would amount to $\sim 10^{-4} M_{\odot}$, which is less than half of that contained in HD 149026b. If debris material plunges into the host star along radial orbits, modest size planetesimals would survive the passage through the convective layer and disintegrate in the radiative region. The amount of disrupted planetesimals in the stellar atmosphere and envelope depends on their trajectory, composition, as well as the background temperature and density distributions. In order to take into account two limiting possibilities, we adopt two simple prescriptions for the deposition of the accreted heavy elements in the polluted stellar models.

We first consider the possibility that the residual planetesimals, embryos, and ill-fated gas giants undergo a gradual orbital decay and enter the stellar envelope through the stellar atmosphere with a large azimuthal motion. In this case, even the largest embryos or gas giant will be completely disrupted in the convective layer (Sandquist et al. 2002). Thus in our first prescription, we assume that the observed metallicity of HD 149026 applies only to its thin convective layer, whereas its interior has a solar metallicity.

In a second prescription, we consider the other possibility that pollutants strike the host star on a direct radial trajectory. This assumption would be appropriate if the debris is scattered into the stellar envelope by close encounters with the gas giant. In this case, it is possible for a considerable amount of pollutants to deposit in the star’s vast radiative envelope below the convective layer. For a swarm of planetesimals falling onto the star, we assume a size distribution of $dN/da \sim a^{-3.5}$ (Wetherill & Stewart 1989). This mass distribution is comparable to those inferred for the asteroids and the Kuiper belt objects and for the impactors of lunar craters (Hartmann 1999). We assume that the residual planetesimals and embryos plunge radially towards the center of the host star. Based on the results of previous simulations of meteoritic impacts on the atmosphere of Venus (Korycansky & Zahnle 2005), we assume that the amount of ablated mass of individual planetesimals is comparable to

the mass of the background gas encountered along the path. Thus, the disruption depth of planetesimals is a function of their sizes.

Given the density distribution of a particular stellar structure, we can integrate to obtain the deposited mass at each layer as a function of the penetrating depth. Fig. 1 shows the mass distribution of $10M_{\oplus}$ pollutants deposited along stellar radius for a $1.3M_{\odot}$ star of an initial solar metallicity at ZAMS. The convective and radiative zones are marked and separated by a vertical dotted line.

For both prescriptions, we consider the possibility that the bombardment of debris may persist for an extended period of time. We assume the accretion begins when the star reaches ZAMS with an initial solar and homogeneous metallicity and the accretion lasts for a duration of 100 Myr. Observations in the mid-IR have shown that the total mass of the grains in the disk declines with time (Rieke et al. 2005). We have thus assumed a time dependence of the rate of planetesimal bombardment suggested by the IR observations. The accretion rate thus declines monotonically as the star evolves.

3. The effect of pollution on the stellar structure

For the first limiting case of the accreted planetesimals’ trajectory, we mix all the heavy elements of the accreted material through the convective zone. In the second case, we still uniformly mixed those material which were ablated in the convective region. While for the relatively large planetesimals penetrating below the convective layer, we added the heavy elements deposited in these regions to the local metallicity distribution in the radiative region. Without a better understanding of the accreted material’s composition, we assume that it contains no hydrogen or helium but has the same composition of heavy elements as that of the star in our calculation. The helium abundance of the host star was deduced using $\frac{\delta Y}{\delta Z} = \frac{Y - Y_{\odot}}{Z - Z_{\odot}} = 2.5$ (Pagel et al. 1992).

In Fig. 2a), we show a comparison between the two limiting pollution prescriptions of the initial metallicity profiles in the outer region of our polluted stellar model. In each case, we assume $\sim 5M_{\oplus}$ debris rocky material is accreted onto a ZAMS host star. From Fig. 1 and Fig. 2a), we find that a considerable amount of the accreted material enters the radiative region in the case that the planetesimals collide the host star in a head-on trajectory. In the following one million year, another $5M_{\oplus}$ rocky material is added. Fig. 2 b) shows the metallicity profiles of the two models at the time of $1 \times 10^8 yr$, when all $10M_{\oplus}$ heavy elemental material has been accreted. At that time, some diffusion has already occurred for both models at the boundary between the convective and radiative regions. Fig. 2c) shows

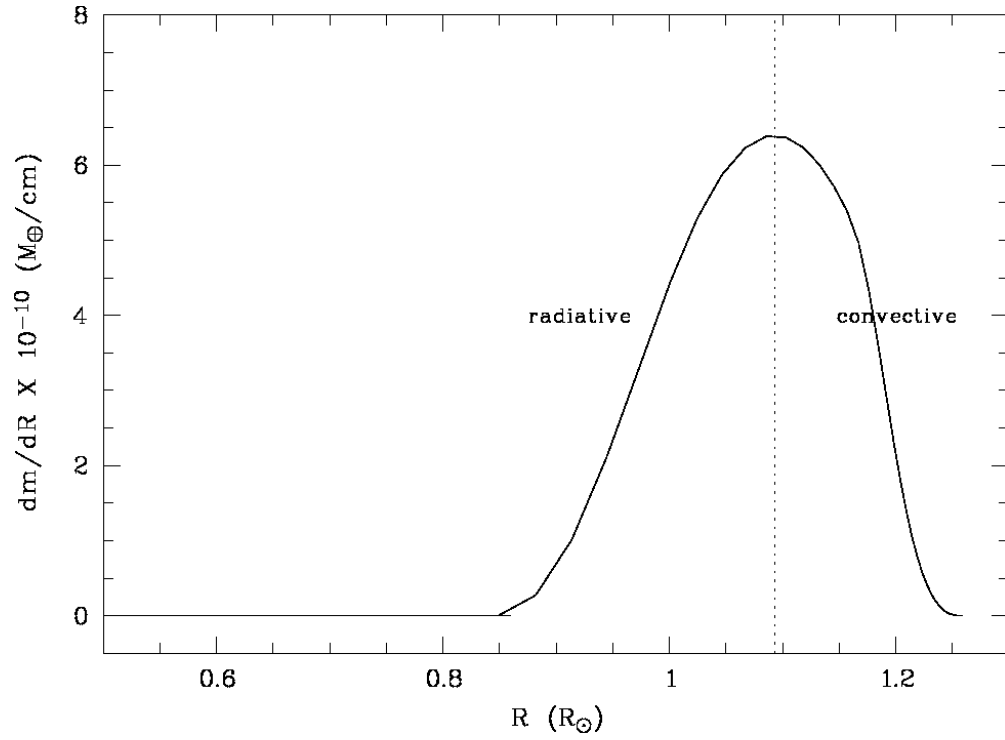


Fig. 1.— Mass distribution of deposited planetesimals along stellar radius. Totally $10 M_{\oplus}$ planetesimals were added to a $1.3 M_{\odot}$ star with an initial solar metallicity at ZAMS.

the metallicity profiles for both models at the time of $3 \times 10^9 yr$, which is approximately the age of HD 149026. Due to the diffusion of heavy elements and the deepening of the surface convective zone, the surface metallicity at this late epoch has decreased considerably in both models.

Fig. 3 shows the evolutionary tracks by adding the accreted material in the two limiting ways. Both models have a mass of $1.3 M_{\odot}$ and an initial solar metallicity. We can find that during the main sequence, especially where the tracks locate within the observational error bars for HD 149026, there is little difference between the two models in luminosity and effective temperature. However, while the model with significant amount of material deposited in the radiative zone can produce a surface metallicity within the observed uncertainties for $[Fe/H]$ of HD 149026, the model with all material mixed in the convective zone has a surface metallicity much larger than the upper limit of the observed $[Fe/H]$. Therefore, the main effect of the metallicity enhancement in the radiative zone compared with that in the convection zone is that it can increase the radiative opacity, redden the star and make it expand without causing significant surface metallicity increase. As HD 149026 has a very shallow surface convective zone, it's more likely that a lot of infalling planetesimals will penetrate into the radiative region. Therefore, we use the second pollution prescription for the following calculations.

4. Evolution of HD 149026

Based on the above definitions of pollution, we construct polluted stellar models for HD 149026 which host a Saturn-mass planet with a large dense core in a 2.8766 day orbit (Sato et al. 2005). Three basic observational parameters are required to constrain our models. From spectroscopic analysis (Sato et al. 2005), the effective temperature T_{eff} and metallicity $[Fe/H]$ for HD 149026 are determined to be 6147 ± 50 K and 0.36 ± 0.05 , respectively. Another important parameter is its luminosity. From the Hipparcos catalog (ESA 1997), the parallax and visual magnitude of HD 149026 are 12.68 ± 0.79 mas and 8.15, respectively. The bolometric correction (BC) is estimated to be -0.026 ± 0.006 by interpolating the effective temperature using the $T_{eff} - BC$ conversion relationship provided by Flower (1996). Then, we arrived at a bolometric luminosity of $2.756_{-0.300}^{+0.363} L_{\odot}$ with 1σ error bar of the parallax. We show below the results of a range of theoretical models with different stellar parameter (such as stellar mass and interior metallicity) that are within the observational uncertainties. For example, a 3σ uncertainty in the parallax-distance determination leads to an uncertainty of $(+1.393, -0.789)L_{\odot}$ in the absolute luminosity of HD 149026.

For the standard model of HD 149026 without pollution (with a homogeneous metallicity

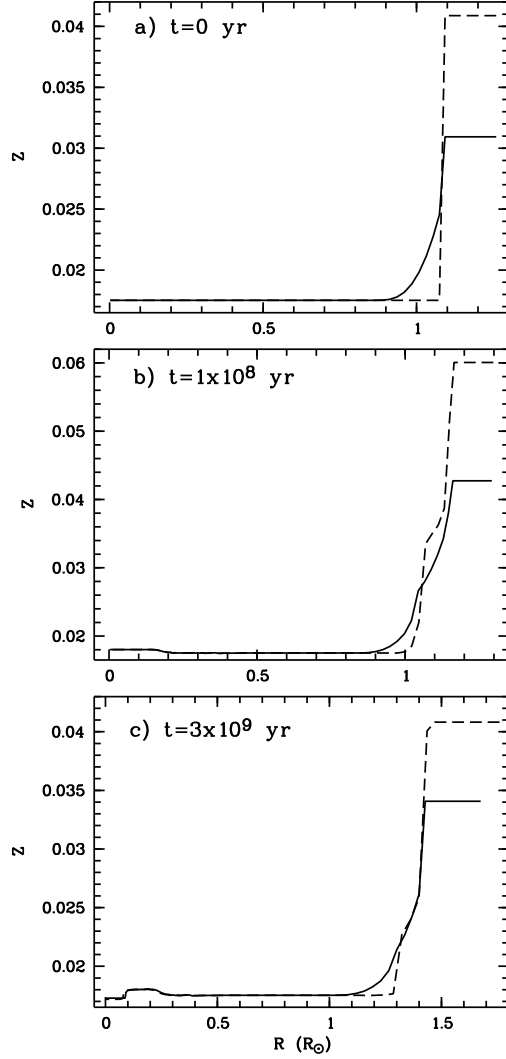


Fig. 2.— Metallicity profiles against stellar radius at different evolutionary times, a) ZAMS, when $\sim 5M_{\oplus}$ is accreted by the star, b) $1 \times 10^8 yr$, when totally $10 M_{\oplus}$ rocky material is added and accretion stops thereafter, c) $3 \times 10^9 yr$. Models polluted by two limiting ways are plotted. The solid line shows the result of our second prescription for the distribution of deposited material as plotted in Fig. 1. While the dashed line corresponds to our first prescription where all infalling material is dissolved and mixed in the convective zone.

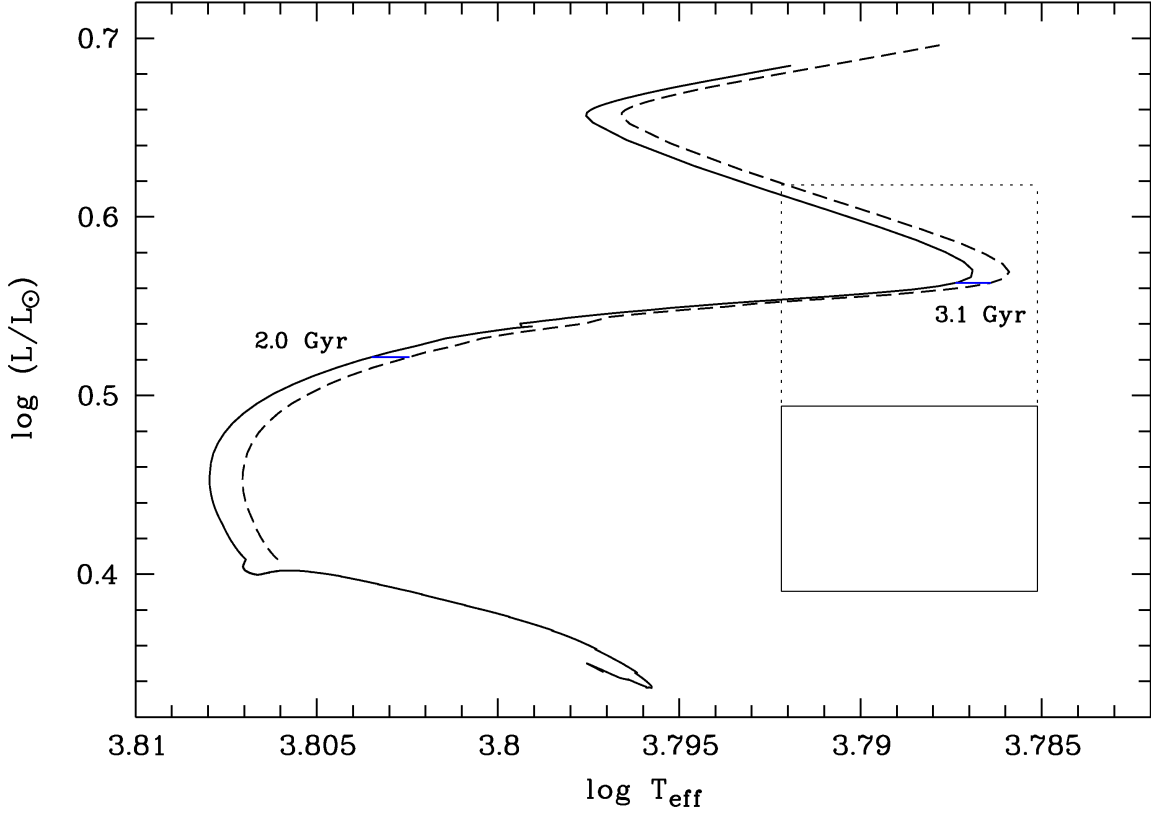


Fig. 3.— Evolutionary tracks of a $1.3 M_{\odot}$ and solar interior metallicity star polluted in two limiting ways. The total amount of accreted material for both models is $10 M_{\oplus}$. Different line types have the same denotations as that in Fig. 2. The solid line box shows 1σ observational errors for luminosity and temperature. The upper limit of luminosity taking into account 3σ error of parallax is shown by the dotted box.

distribution), we obtain a stellar mass of $1.3 M_{\odot}$ and an age of 2.27 Gyr. Around this standard model, we have constructed a series of polluted stellar evolution models with masses in the range of 1.2 to $1.4 M_{\odot}$. Two sets of initial metallicity, solar metallicity and 1.5 times solar metallicity were specified for these models. The models were evolved by accreting different amount of heavy elements.

We firstly illustrate the effect of pollution of the stellar-evolution track in the color-magnitude diagram. In Fig. 4, we show a series of models with $M_* = 1.3 M_{\odot}$ and $Z_* = 1.5 Z_{\odot}$ throughout the star. In this figure, the evolutionary track of a model with an unpolluted homogeneous interior (with 1.5 solar metallicity) is denoted by a thin solid line. Overplotted are the evolutionary tracks of models which are polluted by a total amount $10 M_{\oplus}$, $30 M_{\oplus}$, $50 M_{\oplus}$ and $70 M_{\oplus}$ of heavy elements. Two ages are labeled on the tracks. For comparison, we have also computed the evolutionary track of a $1.3 M_{\odot}$ model with the observed metallicity of HD 149026 (the thick solid line in Fig. 4).

Contrasting these models at any given effective temperature, we find that the accretion of heavy elements decreases the luminosity as a consequence of the opacity enhancement in the radiative layer. The reduced efficiency of radiation transfer also increases the central temperature of the star and speeds up the stellar evolution process. Consequently, at the same age, the surface metallicity enhancement has the general effects of 1) reducing the effective temperature near the main sequence turn off; 2) increasing the stellar radius; and 3) decreasing the luminosity.

5. Observational tests

The accretion of heavy elements increases the metallicity of the surface layer while that in the deep stellar interior retains its initial value. In order to make direct comparison with the observed properties of HD 149026, we need to match the surface metallicity of a series of models with the observed value $[\text{Fe}/\text{H}]=0.36$. This surface boundary condition places a constraint on the extent of heavy-element pollution. Take the $1.3 M_{\odot}$ models with internal $1.5 Z_{\odot}$ for example, the amount of pollution needed to satisfy all the observational constraints (L_* , T_{eff} , and $[\text{Fe}/\text{H}]$) within 1σ error bars is between 10 to $20 M_{\oplus}$.

We note that the relative errors in both $[\text{Fe}/\text{H}]$ and L_* are an order of magnitude larger than that in T_{eff} . We firstly consider the possible range of stellar models. In Fig. 5, We consider a series of models (with different M_*) with initial solar metallicity which is also preserved in the stellar interior. For each mass, the two tracks correspond to the upper and lower limit of metal required to match the observed range in $[\text{Fe}/\text{H}]$. These nearly overlapping

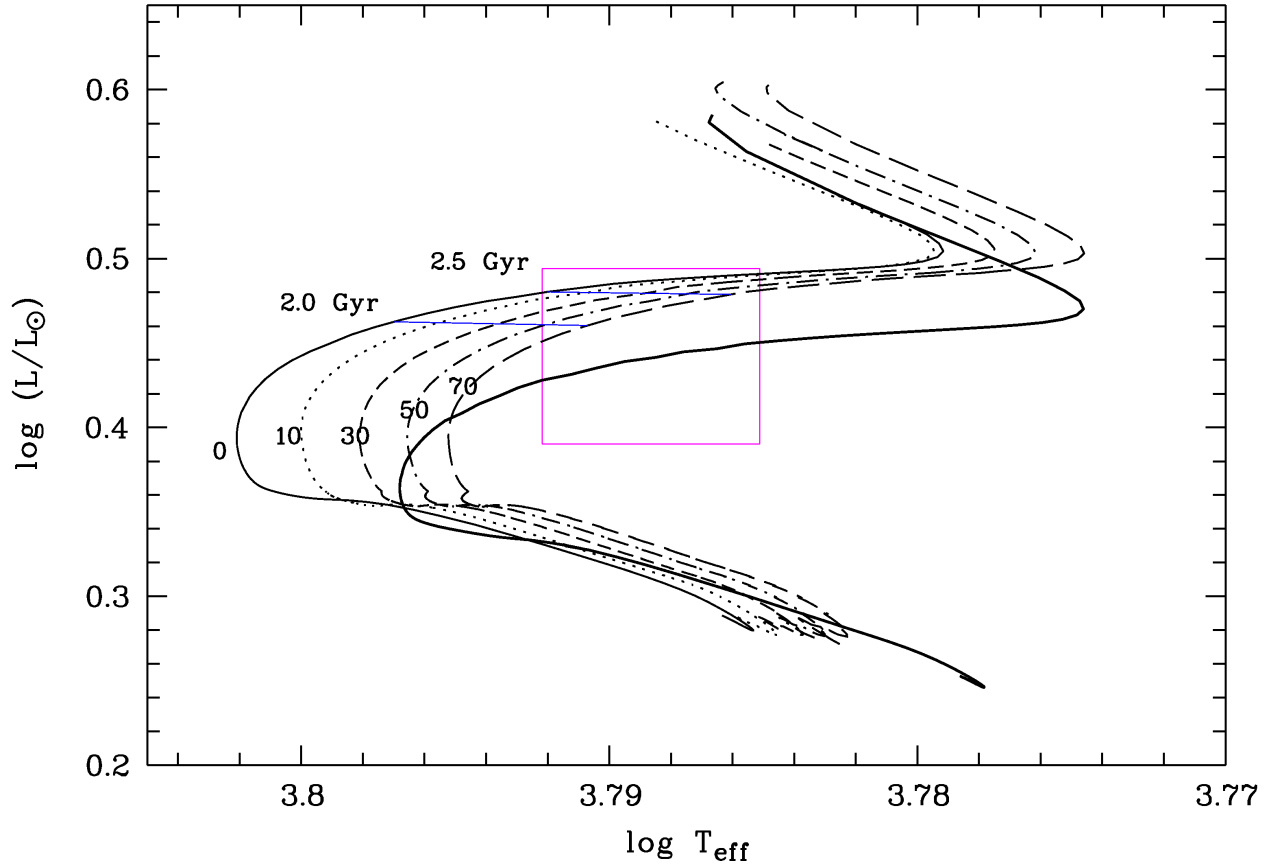


Fig. 4.— The unpolluted models with $1.3 M_{\odot}$ stellar mass and internal 1.5 solar metallicity are plotted in the thin solid line. The tracks marked by different numbers denote different amount of pollution in earth mass based on the unpolluted model. While the model with the mass of $1.3 M_{\odot}$ and observed metallicity of HD 149026 is plotted in thick line for comparison. Overplotted is the 1σ error box for observed effective temperature and luminosity.

tracks indicate that the values of L_* and T_{eff} are more sensitive to M_* than to the exact value of $[\text{Fe}/\text{H}]$. This plot also indicates that the amount of pollution can be constrained quite well by the observed metallicity for a model with the same mass and internal metallicity.

Overplotted in Fig. 5 is the 1σ (solid lines) error box for the observed effective temperature and luminosity. Considering that the stellar distance is difficult to be determined accurately, we extended the error box by taking into account 3σ error of parallax (dotted lines). Models with $M_* > 1.35 M_\odot$ are excluded because they produce over luminous (for the observed range of T_{eff}) tracks. Models with $M_* < 1.15 M_\odot$ are excluded because they produce insufficiently hot T_{eff} (for the observed range of L_*) tracks. A star of $M_* = 1.22 M_\odot$ passes the center of the error bar box. For this particular model, the total amount of pollutant required to bring the surface metallicity to the observed value is $\Delta M_Z \simeq 28 M_\oplus$, which is a significant fraction of the heavy element content in HD 149026b.

We considered another series of models with an initial metallicity equals to 1.5 times that of the Sun (Fig. 6). Obviously, less heavy elements are needed to match the observed $[\text{Fe}/\text{H}]$ than those models in Fig. 5. Models with $1.2 M_\odot < M_* < 1.4 M_\odot$ pass through the extended error box with $M_* = 1.27 M_\odot$ as a best fit, which requires a total amount of pollutant of $\Delta M_Z \simeq 20 M_\oplus$. Note that the unpolluted model in Fig. 4 which matches the most probable observational data has $M_* = 1.3 M_\odot$.

The above results indicate that several models, with or without pollution, can be constructed within the present observational uncertainties. While effective temperature and surface metallicity have been determined quite well by present spectroscopic observations, the current observational uncertainties in luminosity make it difficult to distinguish the models. More accurate luminosity is thus highly desired. We note from Figs. 5 and 6 that stellar mass and internal metallicity are degenerate parameters in determining the evolutionary tracks in H-R diagram, even if stellar luminosity is well constrained. Given independently measured stellar mass with high precision, the internal metallicity of the star can be constrained by fitting the theoretical evolutionary tracks. A definite difference between the internal and surface metallicity in a star is a good evidence of the occurrence of pollution onto this star. Thus, a set of more accurately determined luminosity and independently measured stellar mass, combined with our stellar models, provide a promising way to explore the pollution (if any) history of the star.

The stellar luminosity adopted in our models are calculated using the parallax and visual magnitude obtained from the Hipparcos catalog (ESA 1997). For HD 149026 with a visual magnitude of 8.15, the uncertainty of parallax is ± 0.79 mas. Higher accuracy will be achieved by the European Gaia astrometry mission which is due for launch in 2011. For stars with $V = 10$, the parallax accuracy is expected to be around $7 \mu\text{as}$, which is less

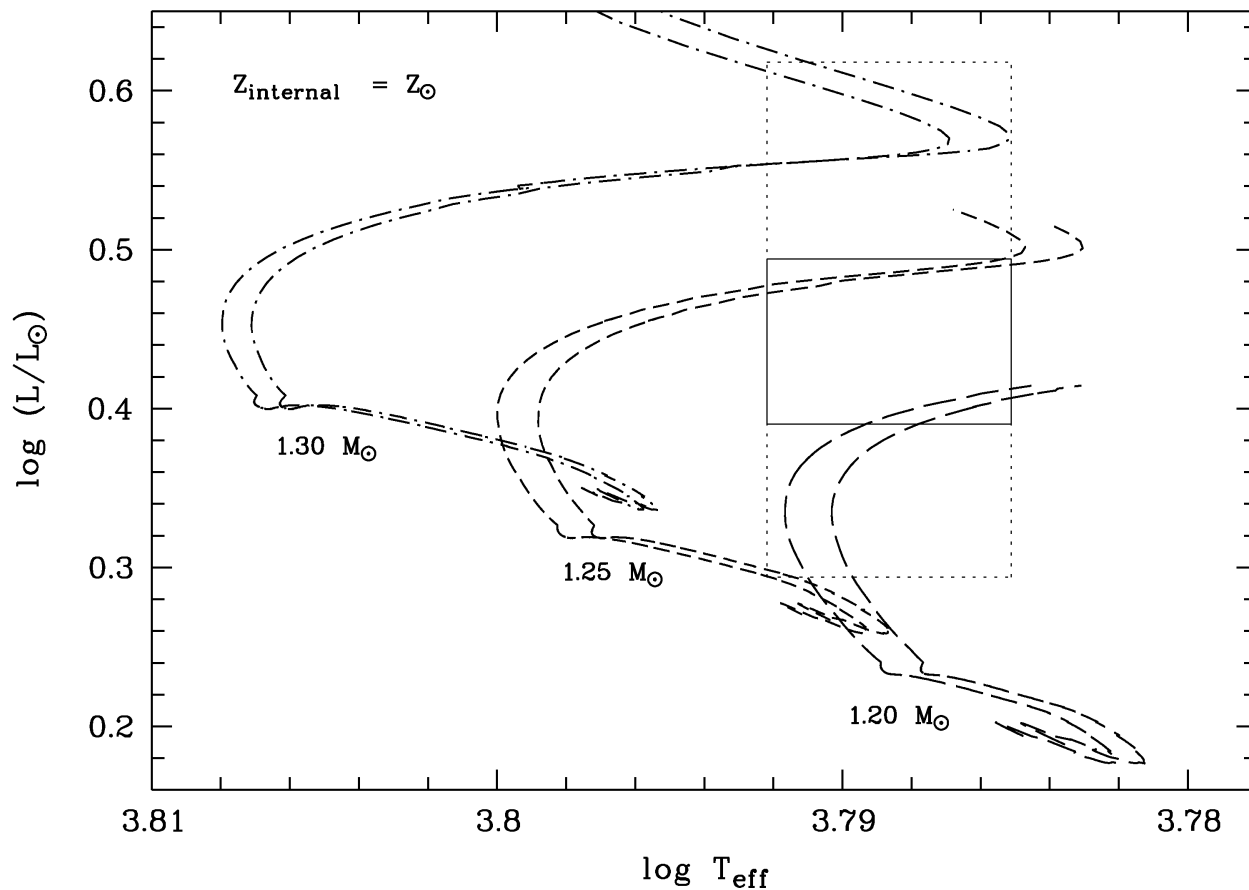


Fig. 5.— Possible polluted models with internal solar metallicity for different stellar masses. For each mass, the two tracks correspond to the upper and lower limit of metallicity that needs to be added to match the observed range in $[\text{Fe}/\text{H}]$. The 1σ error box for observed effective temperature and luminosity is plotted in solid line. While the dotted error box takes into account 3σ error of parallax.

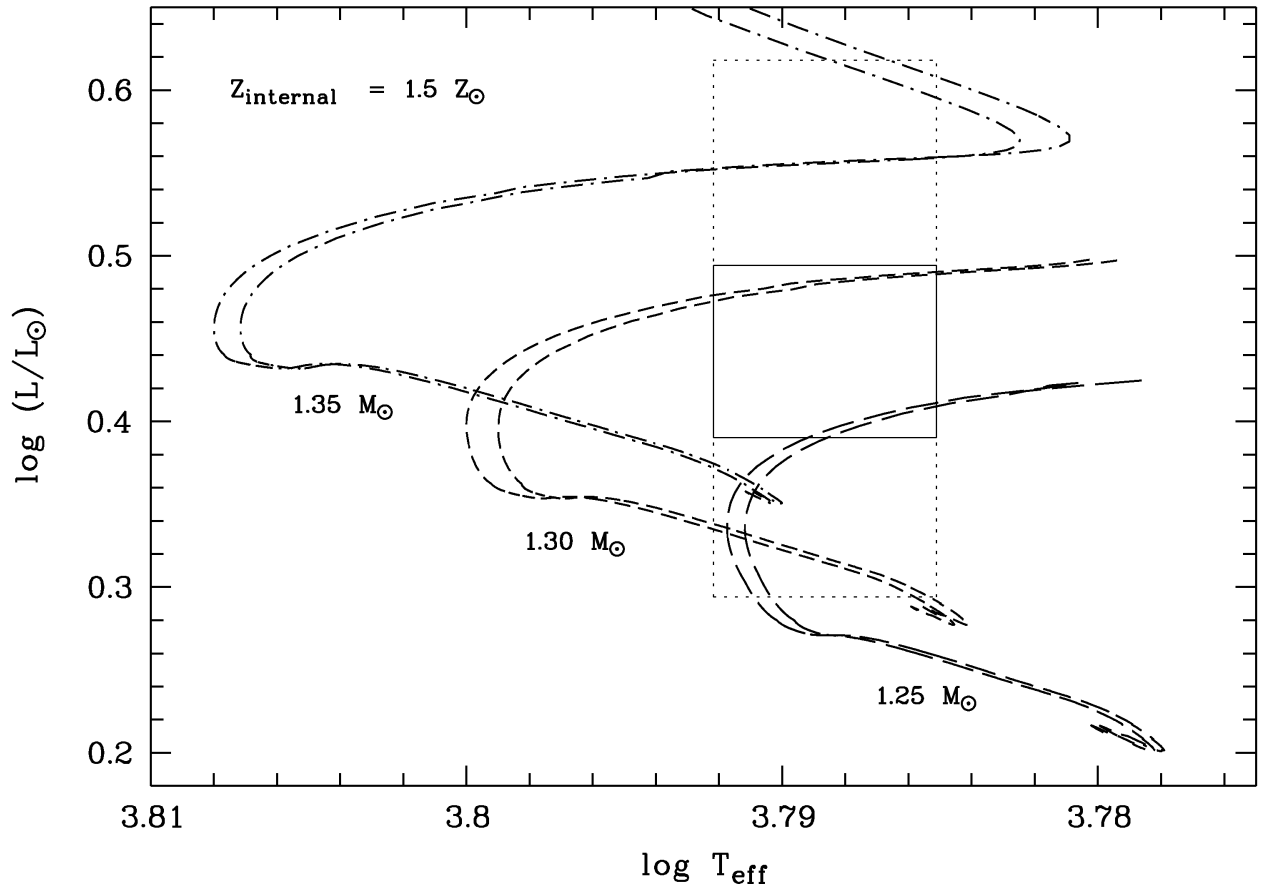


Fig. 6.— Same as Fig. 5, but for possible polluted models with an internal metallicity of 1.5 times solar.

than 1% of present observational uncertainty (Jordi et al. 2006). This improvement reduces the uncertainty in luminosity by a factor of 30. In this case, if the stellar mass can be determined independently with an accuracy of $\sim 1\%$, it's possible that the polluted and unpolluted models are distinguishable.

However, it is a big challenge to measure stellar mass precisely. Usually, stellar mass can be determined in binary systems using astrometric methods. For eclipsing binaries, an accuracy of 2-3% can be achieved in the best case (Balega et al. 2007). For single stars with a planetary companion, it is possible to determine the stellar mass if the planet transits the star. By solving the equations of transit geometry and Kepler's third law, the average stellar density can be derived as

$$\rho_* = \frac{32P}{\pi G} \frac{\Delta F^{3/4}}{(t_T^2 - t_F^2)^{3/2}} \quad (1)$$

where t_T is the total transit duration, t_F is the duration of the transit completely inside ingress and egress, P is the period, and ΔF is the transit depth (Seager & Mallén-Ornelas 2003; Gillon et al. 2006; Winn 2007). The stellar radius can be determined independently by using the Stefan-Boltzmann law, rather than the isochrone fitting method (Sato et al. 2005). Combined with ρ_* calculated from the transit light curve, the stellar mass M_* can be obtained independently. At present, the stellar density can be constrained to 3% by HST observation (Pont et al. 2007). Also, the stellar radius can be constrained better by the improved luminosity measurement. Thus, it's possible that the stellar mass can be obtained with a marginal accuracy as required to test our theoretical models.

Gravitational microlensing is another promising method to determine the stellar mass of single stars accurately. Paczynski (1998) shows that it's possible for the Space Interferometry Mission (SIM) to measure M_* of nearby stars with an accuracy of 1% using this method.

With the aforementioned upcoming high-precision astrometry missions, we expect that our theoretical stellar models will be able to test whether pollution is a significant effect inducing the high metallicities of stars with planets. Another direct probe for testing the occurrence of pollution is associated with the modification in the internal structures and the oscillation frequencies of the stars. In Figs. 7 and 8, we plot the density and temperature distribution in the stellar envelope for three best-fit models (with initial and internal $[\text{Fe}/\text{H}] = 0, 0.15, \text{ and } 0.36$, and stellar mass $M_* = 1.22M_\odot, 1.27M_\odot, \text{ and } 1.3M_\odot$ respectively). We will consider elsewhere the difference in the g-mode oscillation frequency associated with the dispersion in the structure of these models.

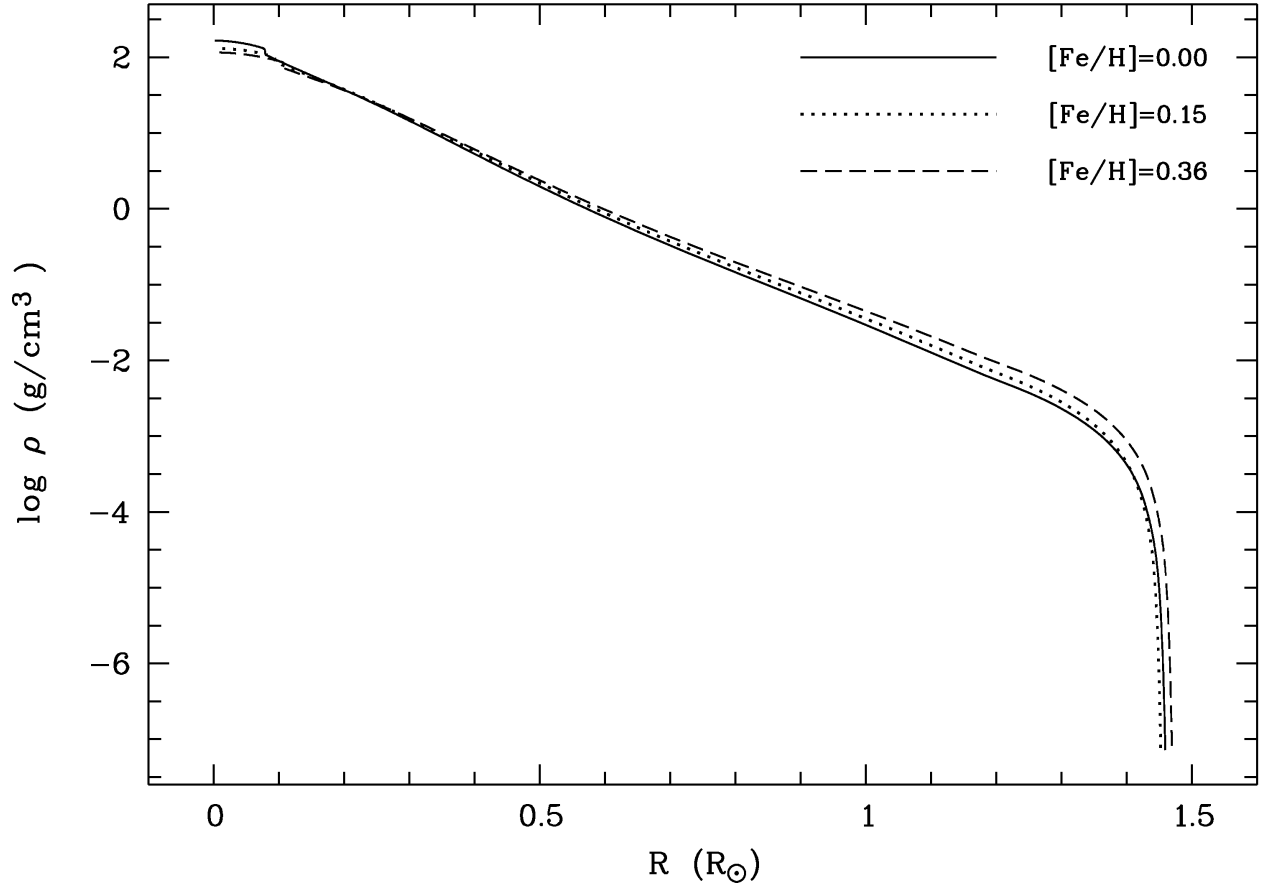


Fig. 7.— Density profiles for the three best-fit models, with stellar mass $M_* = 1.22M_{\odot}$ and initial $[\text{Fe}/\text{H}] = 0$ (solid line), $M_* = 1.27M_{\odot}$ and $[\text{Fe}/\text{H}] = 0.15$ (dotted line), and $M_* = 1.3M_{\odot}$ and $[\text{Fe}/\text{H}] = 0.36$ (dashed line), respectively.

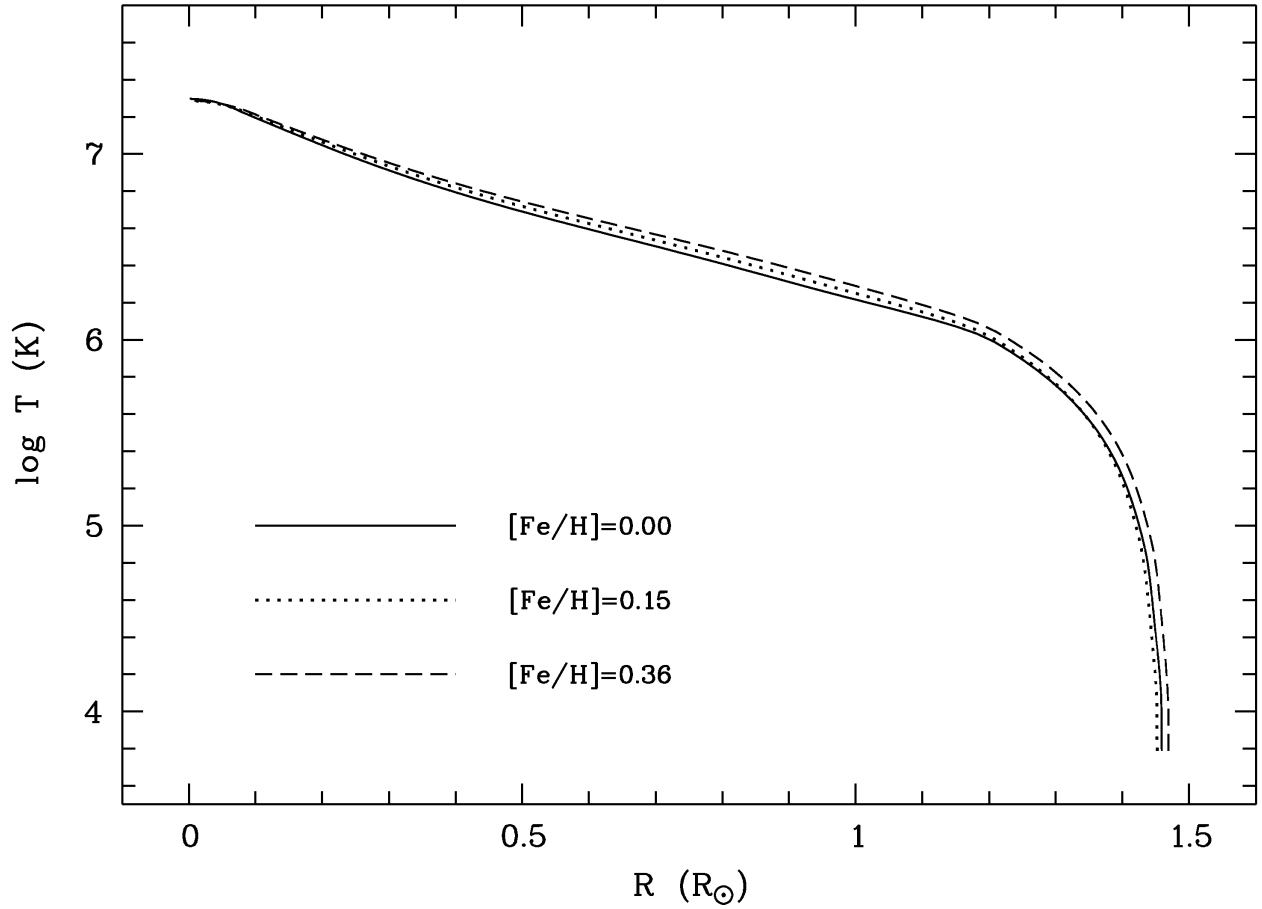


Fig. 8.— Temperature profiles for the three best-fit models, with stellar mass $M_* = 1.22M_\odot$ and initial $[\text{Fe}/\text{H}] = 0$ (solid line), $M_* = 1.27M_\odot$ and $[\text{Fe}/\text{H}] = 0.15$ (dotted line), and $M_* = 1.3M_\odot$ and $[\text{Fe}/\text{H}] = 0.36$ (dashed line), respectively.

6. Summary and Discussions

In this paper, we considered the possibility that the outer envelope of a metal-rich planet-bearing star HD 149026 may have been significantly polluted by residual planetesimals or some gas giant planets. This system is particularly interesting because it contains a planet with most of its mass in its core and an intermediate-mass star which has recently entered the post main sequence evolutionary phase. In a subsequent paper, we will suggest that this large-core Saturn-mass planet HD 149026b was formed through giant impacts onto a proto gas giant planet by either residual protoplanetary embryos or by other gas giant planets in the proximity of the host star. A significant fraction of metal of the building blocks may not merge or be retained as a consequence of grazing high-velocity collisions. However, those debris may undergo orbital decay or remain in the close proximity of HD 149026b.

We assume that a substantial fraction of the original residual planetesimals in the neighborhood of HD 149026b may have been scattered into its host star which is an F stars with a very shallow convective layer. We carried out evolution calculations to take into account the effect of stellar pollution. We suggest that in this and other F star with planets, the extent of stellar pollution by residual planetesimals may be tested by accurate determinations of their mass, luminosity, and effective temperature. Such accurate measurements, when combined with an accurate transit light curve, may provide a firm support on the stellar accretion of a substantial population of terrestrial-planet-building material as well as one or more gas giant planets similar to HD 149026b.

We thank Drs C. Agnor, P. Bodenheimer, L. C. Deng, D. Korycansky, and E. Sandquist for useful conversation. This work is supported by NASA (NAGS5-11779, NNG04G-191G, NNG06-GH45G, NNX07AL13G, HST-AR-11267), JPL (1270927), and NSF(AST-0507424).

REFERENCES

- Adams F. C., Laughlin G., 2003, *Icarus*, 163, 290
- Alexander D. R., Ferguson J. W., 1994, *ApJ*, 437, 879
- Bahcall J. N., Pinsonneault M. H., Wasserburg G. J., 1995, *Reviews of Modern Physics*, 67, 781
- Balega Y. Y., Beuzit J. L., Delfosse X., Forveille T., Perrier C., Mayor M., Ségransan D., Udry S., Tokovinin A. A., Schertl D., Weigelt G., Balega I. I., Malogolovets E. V., 2007, *A&A*, 464, 635

- Christensen-Dalsgaard J., Gough D. O., Thompson M. J., 1991, *ApJ*, 378, 413
- Cody A. M., Sasselov D. D., 2005, *ApJ*, 622, 704
- Dollinger M. P., Hatzes A. P., Pasquini L., Gyenther E. W., Hartmann M., Girardi L., Esposito M., 2007, *A&A*, 472, 649
- Dotter A., Chaboyer B., 2003, *ApJ*, 596, 496
- Eggleton P. P., 1971, *MNRAS*, 151, 351
- Eggleton P. P., 1972, *MNRAS*, 156, 361
- ESA, 1997, *The Hipparcos and Tycho Catalogues (ESA Sp-1200)*. ESA, Noordwijk
- Fischer D. A., Valenti J. A., 2003, in *Scientific Frontiers in Research on Extrasolar Planets*, eds. Deming D. & Seager S. (San Francisco: ASP), ASP conf. Ser., 294, p. 117
- Fischer D. A., Valenti J., 2005, *ApJ*, 622, 1102
- Flower P. J., 1996, *ApJ*, 469, 355
- Ford E. B., Rasio F. A., Sills A., 1999, *ApJ*, 514, 411
- Garaud P., Lin D. N. C., 2004, *ApJ*, 608, 1050
- Gillon M., Pont F., Moutou C., Bouchy F., Courbin F., Sohy S., Magain P., 2006, *A&A*, 459, 249
- Goldreich P., Tremaine S., 1980, *ApJ*, 241, 425
- Gonzalez G., 1997, *MNRAS*, 285, 403
- Guenther E. W., Paulson D. B., Cochran W. D., Patience J., Hatzes A. P., Macintosh B., 2005, *A&A*, 442, 1031
- Hartmann W. K., 1999, *Moons and Planets*, the 33rd Symposium on Celestial Mechanics, 4th Edition. Wadsworth, Belmont
- Heppenheimer T. A., 1980, *Icarus*, 41, 76
- Ida S., Lin D. N. C., 2004, *ApJ*, 604, 388
- Ida S., Lin D. N. C., 2005a, *ApJ*, 626, 1045
- Ida S., Lin D. N. C., 2005b, *Prog. Theor. Phys. Suppl.*, 158, 68

- Ida S., Lin D. N. C., 2007, astro-ph/0709.1375
- Iglesias C. A., Rogers F. J., 1996, ApJ, 464, 943
- Korycansky D. G., Zahnle K. J., 2005, Planet. Space Sci., 53, 695
- Johnson J. A., Butler R. P., Marcy G. W., Fischer D. A., Vogt S. S., Wright J. T., Peek K. M. G., 2007, ApJ, 670, 833
- Jordi C., Høg E., Brown A. G. A., Lindegren L., Bailer-Jones C. A. L., Carrasco J. M., Knude J., Straizys V., de Bruijne J. H. J., Claeskens J. F., Drimmel R., Figueras F., Grenon M., Kolka I., Perryman M. A. C., Tautvaišienė G., Vansevičius V., Willemsen P. G., Bridžius A., Evans D. W., Fabricius C., Fiorucci M., Heiter U., Kaempf T. A., Kazlauskas A., Kučinskas A., Malyuto V., Munari U., Reylé C., Torra J., Vallenari A., Zdanavičius K., Korakitis R., Malkov O., Smette A., 2006, MNRAS, 367, 290
- Laughlin G., Adams F. C., 1997, ApJ, 491, L51
- Li S.-L., Agnor C., Lin D. N. C., 2007, in preparation
- Lin D. N. C., Bodenheimer P., Richardson D. C., 1996, Nature, 380, 606
- Lin D. N. C., Papaloizou J., 1986, ApJ, 309, 846
- Livio M., Soker N., 2002, ApJ, 571, L161
- Masana E., Jordi C., Ribas I., 2006, A&A, 450, 735
- Nagasawa M., Ida S., 2000, AJ, 120, 3311
- Nagasawa M., Ida S., Lin D. N. C., 2001, in Kokubo E., Ito T., Arakida H., eds, *the 33rd Symposium on Celestial Mechanics, 2001: a symplectic odyssey*. Mitaka, Tokyo, Japan, p. 148
- Nagasawa M., Lin D. N. C., 2005a, ApJ, 632, 1140
- Nagasawa M., Lin D. N. C., Thommes E., 2005b, ApJ, 635, 578
- Ogilvie G. I., Lin D. N. C., 2007, ApJ, 661, 1180
- Paczynski B., 1998, ApJ, 494, L23
- Pagel B. E. J., Simonson E. A., Terlevich R. J., Edmunds M. G., 1992, MNRAS, 255, 325

- Pasquini L., Döllinger M. P., Weiss A., Girardi L., Chavero C., Hatzes A. P., da Silva L., Setiawan J., 2007, *A&A*, 473, 979
- Pols O. R., Tout C. A., Eggleton P. P., Han Z., 1995, *MNRAS*, 274, 964
- Pont F, Gilliland R. L., Moutou C., Charbonneau D., Bouchy F., Brown T. M., Mayor M., Queloz D., Santos N., Udry S., 2007, *A&A*, 476, 1347
- Rieke G. H., Su K. Y. L., Stansberry J. A., Trilling D., Bryden G., Muzerolle J., White B., Gorlova N., Young E. T., Beichman C. A., Stapelfeldt K. R., Hines D. C., 2005, *ApJ*, 620, 1010
- Rogers F. J., 1994, in Chabrier G., Schatzman E., eds, *IAU Colloquium 147, The Equation of State in Astrophysics*. Cambridge Univ. Press, Cambridge, p. 16
- Sandquist E. L., Dokter J. J., Lin D. N. C. Mardling R. A., 2002, *ApJ*, 572, 1012
- Santos N. C., Israelian G., Mayor M., Rebolo R., Udry S., 2003, *A&A*, 398, 363
- Sato B., Fischer D. A., Henry G. W., Laughlin G., Butler R. P., Marcy G. W., Vogt S. S., Bodenheimer P., Ida S., Toyota E., Wolf A., Valenti J. A., Boyd L. J., Johnson J. A., Wright J. T., Ammons M., Robinson S., Strader J., McCarthy C., Tah K. L., Minniti D., 2005, *ApJ*, 633, 465
- Sato B., Izumiura H., Toyota E., Kambe E., Takeda Y., Masuda S., Omiya M., Murata D., Itoh Y., Ando H., Yoshida M., Ikoma M., Kokubo E., Ida S., 2007, *ApJ*, 661, 527
- Saumon D., Chabrier G., van Horn H. M., 1995, *ApJS*, 99, 713
- Seager S., Mallén-Ornelas G., 2003, *ApJ*, 585, 1038
- Sekiya M., 1983, *Prog. Theor. Phys.*, 69, 1116
- Shen Z.-X., Jones B., Lin D. N. C., Liu X.-W., Li S.-L., 2005, *ApJ*, 635, 608
- Supulver K. D., Lin D. N. C., 2000, *Icarus*, 146, 525
- Thoul A. A., Bahcall J. N., Loeb A., 1994, *ApJ*, 421, 828
- Ward W. R., 1981, *Icarus*, 47, 234
- Ward W. R., 1984, in *Planetary rings*, eds. Greenberg R. & Brahic A. (Tucson: Univ. of Arizona Press), 660
- Ward W. R., Colombo G., Franklin F. A., 1976, *Icarus*, 28, 441

Wetherill G. W., Stewart G. R., 1989, *Icarus*, 77, 330

Wilden B. S., Jones B. F., Lin D. N. C., Soderblom D. R., 2002, *AJ*, 124, 2799

Winn J. N., 2007, [astro-ph/0710.1098](#)

Youdin A. N., Shu F. H., 2002, *ApJ*, 580, 494

Zhou J. L., Aarseth S. J., Lin D. N. C., Nagasawa M., 2005, *ApJ*, 631, L85